Three Gorges Dam Monitoring by Means of Temporal SAR Image Series Analysis

Teng Wang[1,2], Daniele Perissin[1,3], Mingsheng Liao[2], and Fabio Rocca[1]

1, Dipartimento di Elettronica e Informazione, Politecnico di Milano, Milan, Italy
2, LIESMARS, Wuhan University, Wuhan, China
3, Institute of Earth and Information Science, Chinese University of Hong Kong, Hong Kong, China

Abstract:

The Three Gorges Dam, the largest hydroelectric project in the world, is one of the most significant projects in China. In this paper, We measure and analyze the deformation of the Three Gorges Dam and surrounding area with 40 SAR images acquired from 2003 to 2008. We find that the temporal deformation of the left part of the dam stopped since 2003, the deformation being influenced by the changing level of the Yangtze River. The seasonal dilation caused by temperature can be observed as well. The results we obtained fit well with the published results of the Three Gorges Dam deformation measured by conventional survey methods. On the other hand, incoherent information such as the amplitude of the radar signal are also analyzed in the temporal data series. Since the images were acquired during the construction of the dam, an amplitude matrix analysis is proposed to estimate the life span of each target in different parts of the dam. Therefore, whether the dam was releasing water during the satellite pass or not can be detected as well.

1. INTRODUCTION

Nowadays, China is in an era of rapid urbanization and infrastructure construction, many huge man-made projects have been constructed. The Three Gorges Project (TGP), the largest hydroelectric project in the world, is one of the most significant constructions in China. The three main functions of TGP, namely, flood control, power generation and navigation capability enhancement have been bringing about economic, social and environmental benefits. After the construction of the dam, a 660km reservoir has been formed. Due to the high pressure of the reservoir on the riverbed and the water infiltration affection, there exist potential crust instability along the Yangtze. The earth crust structure and the dynamic variations of the gravity field in this area have been studied after the river was blocked [1], [2].

Indeed, deformation is unavoidable for each dam, however, it is very risky for a dam when the displacement overtakes certain threshold. Since the safety of the Three Gorges Dam relates to millions of people living in the downriver plains, the stability monitoring is extremely important. Since the dam deformation happens with millimetric level, high precision deformation survey methods are needed. Although nowadays dam deformation monitoring systems are capable to obtain reliable measures, it is still obligatory to install and maintain monitoring stations [3]. Moreover, conventional survey methods are usually time and human power consuming. Therefore, it is difficult to improve the density of measurement points.

As coherent imaging radars working in microwave frequencies, spaceborne Synthetic Aperture Radars (SAR) have the ability to acquire data with large coverage in all conditions (day-night-free, weather-free). With regular revisiting cycle and highly precise deformation monitoring capability, temporal analysis of space-borne SAR data are very suitable for the task at hand. In the late 1990s Permanent Scatterers InSAR (PS-InSAR) technique was proposed and then became a widely used method to precisely measure the earth deformation from spaceborne SAR images[4], [5]. PS-InSAR technique achieves millimetric level ground deformation monitoring [6], [7] and thus allows monitoring the dam from satellites. However, information hidden in distributed targets that decorrelate in both temporal and spatial domains has to be abandoned. As a consequence, applications of the PS technique are restricted in the areas where less stable point-like targets are available. Aiming at extracting more information from time series SAR data, the Quasi-PS (QPS) technique was presented by considering different interferometric combinations [8]. Since there exist both stable point-like artificial targets and distributed targets in the Three Gorges Dam site, we carry out both analysis in order to gain benefits from the number of points and the accuracy of measurements.

2. TEST SITE AND DATA SETS

The Three Gorges Dam is located near San DouPing town, about 40km from Yi Chang city, in Hubei province. Different parts of the dam are shown in Figure 1. Within the Three Gorges Dam area, there exist bare land, hills, body of the dam, ship locks and other natural and artificial targets. The main structure of the TGP consists of three parts: the dam, hydrological generator plants and navigation instruments. The body of the dam is 2355m long and 185m high. Bottom and top of the dam are respectively 115m and 40m wide. The spillway is in the middle of the dam where the main river canal was. The 23 sluice gates installed on the bottom of the dam are used to control the capability of the upstream reservoir and wash the alluvial sands to the downstream area. The power planthouses, flanking the spillway (left and right riverbank), accommodate altogether 26 sets of turbine-generators. The first generator on the left riverbank planthouse began to function in 2003, and the construction of the right riverbank was finished in 2008. The navigation part of the Three Gorges Project was built on the left riverbank and consist of permanent ship locks and ship lift.

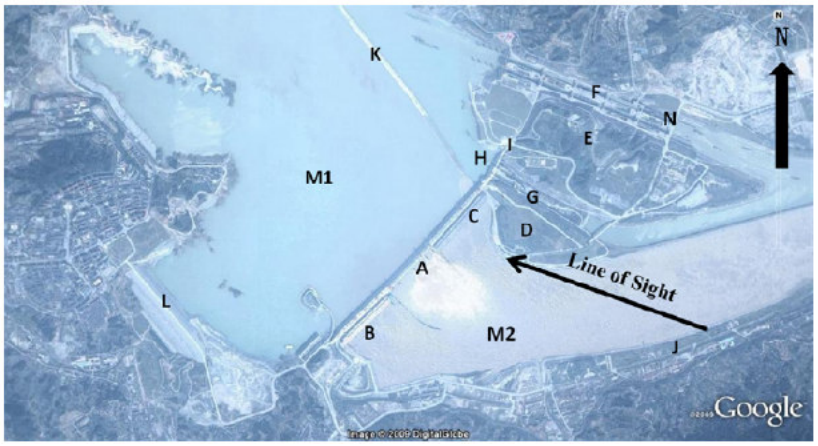

Figure 1 The studied area over Three Gorge Dam site. The optical image is taken from Google Earth. A: Spillway, B: right planthouse, C: Left planthouse, D: Dam view site, E: Tanziling hill, F: Permanent ship lock, G: Temporal ship lock, H: Ship lift, I: 185m elevation platform, J: Memory park, K: Dyke, L: Dike, M1: The Yangtze River (upriver) M2: The Yangtze River (downriver), N: Ship lock view site

In this paper, 40 scenes of Evisat ASAR images, acquired from August 2003 to April 2008, are processed. Figure 2 shows the images acquisition dates and corresponding upriver water level. From Figure 2 we can find that before the first image was acquired in 2003, the water level increased near 90m in a short time, and in the middle of 2006 the water level increased again about 20m. In the following discussions, we analyze the impact of different water levels on the stability of the dam from the time series InSAR results.

Figure 3 shows the incoherent mean amplitude calculated from 40 SAR scenes. Since the satellite line of sight (LOS) is directed towards the downriver part of the dam (see Figure 1), power plants, spillways and the body of the dam can be observed by the satellite. According to the time span and construction progress of the project, the right part of the dam (part B in Figure 1 and Figure 3) was under construction during the time span of our data set. As a consequence, in the mean amplitude image in Figure 3 the targets of the construction site and the cofferdam that was dismounted in June 2006 can still be seen.

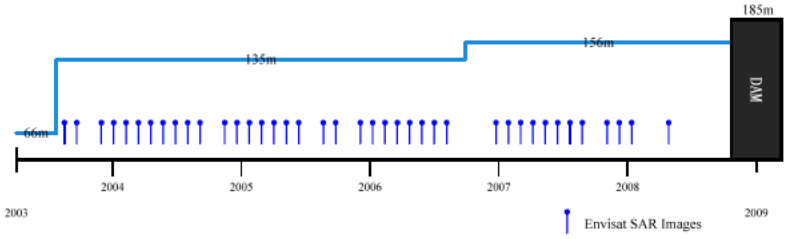

Figure 2 Envisat data acquisition time and corresponding water levels.

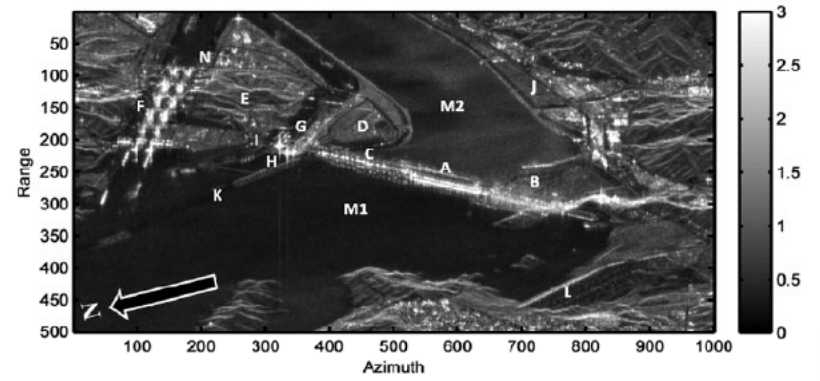

Figure 3 Incoherent amplitude mean of time series SAR images, the letters have the same meaning as in Figure 1

3. TIME SERIES INSAR ANALYSIS RESULTS

3.1 QPS Results

As shown in Figure 4, high temporal coherence is achieved by the QPS algorithm. The left and top parts of the dam show very high coherence due to the temporal stability and strong reflectivity. Moreover, except for the vegetated areas, the stable distributed targets such as Tanziling hill and the upriver bank dike also show high coherence. On the contrary, the spillway, the navigation instruments and the right part of the dam show low temporal coherence. Depending on the normal and temporal baseline distribution, 0.75 is set as our threshold to select QPS points. Within the 60km^2 area, 11463 QPS are detected, and their elevation and deformation information are shown in Figure 5 and Figure 6.

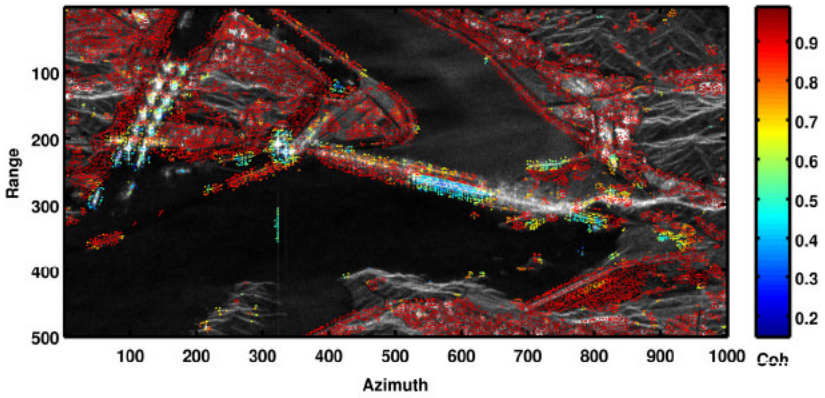

Figure 4 Temporal coherence obtained by QPS technique. The background is the amplitude mean values of processed SAR images.

Since we cannot find any published elevation in this area, the validation of the results are carried out by comparing the results on some known locations: 1) the tail water platform of the left part of the dam is 83.5m, 2) the top of the left planthouse is 117.2m, 3) the top of the dam is 185m, 4) the spillway weir is 158m. From the letters indicated in Figure 3, the estimated elevation from QPS technique fit close to the ground truth. In addition, since the downriver part of the dam faces the satellite LOS, the elevation of the left dam can be represented as three parts: the tail water platform, the top of the planthouse, and the top of the dam. The lifting equipments on the top of the dam show about 200m elevation. Near the

permanent ship locks, although not so many QPS points are present, the five levels of the ship locks can be observed.

From the results shown in Figure 6, over the dam, only slight deformation trends can be observed. In other words, the Three Gorges Dam is quite stable during the time span of our data set. There exist three factors for the deformation of a dam [9]: 1) the water pressure related deformation, 2) the temperature related deformation, 3) the temporal subsidence. In detail, the water pressure related deformation is caused by the pressure of the upriver reservoir towards down and downriver directions, the temperature related deformation is caused by thermal dilation, and the temporal subsidence is caused by the pressure over the earth crust from the new-built dam. As stated in [10], since the left part of the Three Gorges Dam was constructed in 2003, the temporal subsidence caused by the weight of the dam stopped and the basement of the dam has become stable. Since the accuracy of the deformation series is reduced by the selected short temporal baseline interferograms, here, we only analyze water pressure related deformation trends from the QPS results and we analyze the relations between deformation and different water levels according to the PS results.

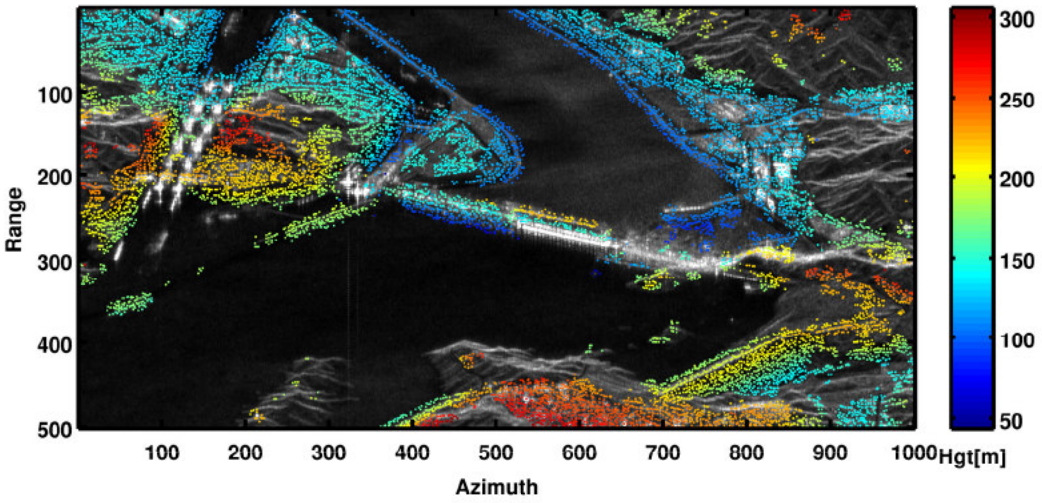

Figure 5 The measured elevation on QPS, the threshold to select QPS is 0.75.

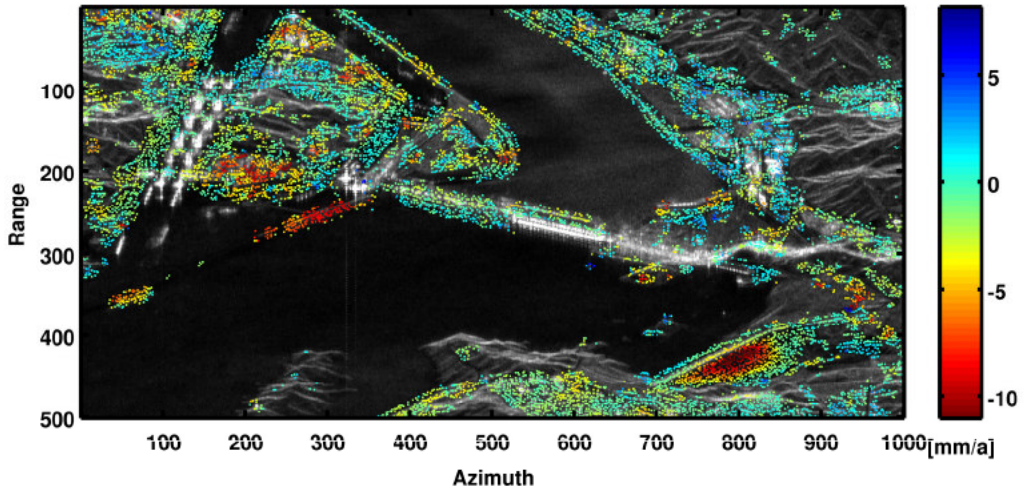

Figure 6 The measured deformation on QPS, the threshold to select QPS is 0.75.

As shown in Figure 7, there exist three kinds of water pressure related deformation: 1) the upriver reservoir presses the earth crust and inclines the basement of the dam towards the upriver direction, 2) the upriver reservoir pushes the dam towards the downriver direction 3) flexibility deformation caused by the upriver pressure. From the results shown in Figure 6, on the top of the left part of the dam, the slight deformation trends are apart from the satellite, on the contrary, the planthouses, on the bottom of

the dam show the deformation trends towards the satellite. According to the different deformation types shown in Figure 7, we presumed that the dam declined slightly on account of the upriver water pressure over the riverbed crust (as shown in Figure 7 (a)).

In the dam surroundings, we detected several subsidence areas in the left riverbank, especially along the axis of the dam to the area between the ship lift and permanent ship locks. We presume that the construction of the navigation establishments changed the distribution of the underground water and caused superficial subsidence. In addition, several slight subsidence areas can be observed near the Yangtze River. Synthetically, superficial subsidence often happens near the water area of Yangtze, the maximum subsidence appears on the upriver embankment near Zigui county. The highest subsidence velocity is over 10mm/year.

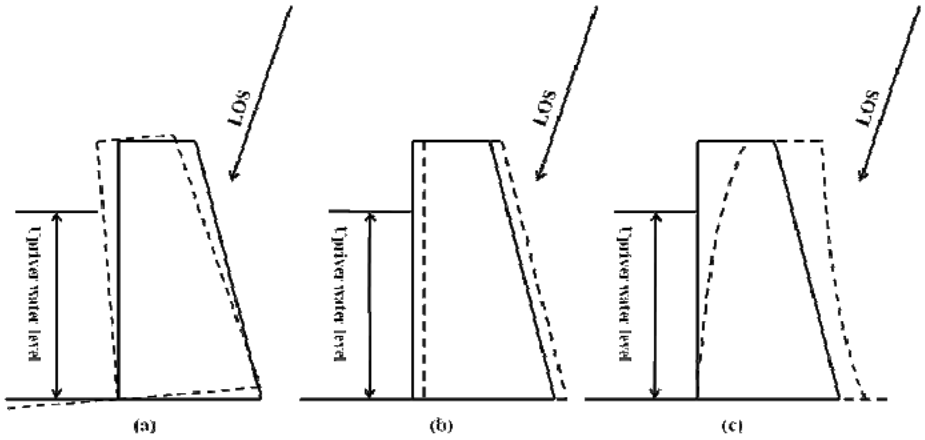

Figure 7 Three types of dam deformation caused by the pressure of water. The arrow indicates the radar looking direction. (a) the upriver reservoir presses the earth crust and makes the basement of the dam incline, thus the dam inclines towards the upriver direction, (b) the upriver reservoir pushes the dam towards the downriver direction. (c) flexibility deformation caused by the horizontal upriver pressure.

3.2 PS Results

From the QPS results, we can presume that the temporal subsidence of the dam almost stopped after the construction of concrete building. Therefore, water pressure and temperature are the main factors of the dam deformation. Figure 9 (a) and (b) show the time series residual phases of two PS on the dam. Figure 9 (a) indicates a target on the top of the dam, (b) indicates a target on the tail water platform. Figure 9 (c) and (d) show the up-down water level difference and upriver water level respectively on the data acquisition time, from which similar trends can be observed. The three red dashed lines in Figure 9 indicate the time when the up-downriver water level difference reached local maximum values and divide the time span into four parts, indicated as I-IV. The red triangle shows the time point when the cofferdam was dismounted.

From the deformation indicated with the PS residual phases, during the time spans I-III, when the upriver rose to the highest values, remarkable deformation is detected by the PS technique, though after several months running, the deformation became smooth. While, after dismounting the cofferdam on the right part dam in June 2006, the Three Gorges Dam tested successfully in running at 156m high water level, the stability of the dam in this period was reduced and shake-like deformation can be observed from the PS results. In addition, the seasonal deformation caused by thermal dilation can also be observed in each stable period.

By synthesizing the QPS and PS measures in the period from 2003 to 2008, we presume that the left part of the Three Gorges Dam declined slightly towards the upriver on account of the upriver water pressure over the riverbed crust. The subsidence of the dam stopped and only slight deformations caused by different water levels and temperatures can be detected. The results fit close to the published Three Gorges Dam deformation monitoring result [10].

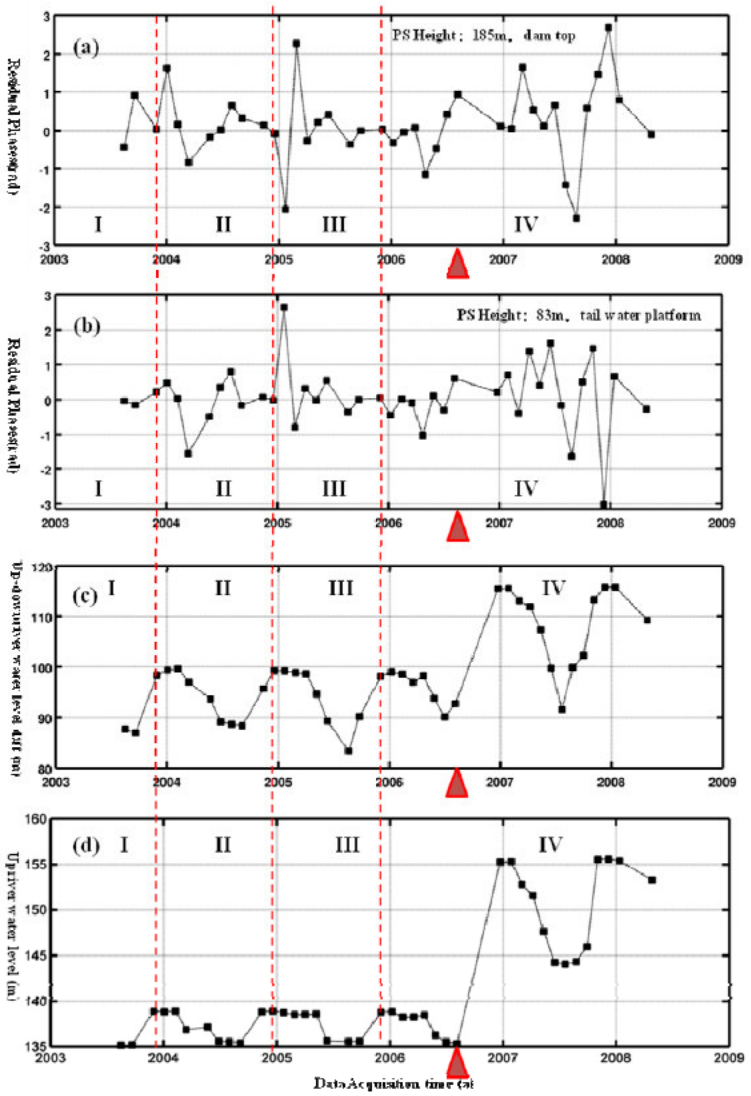

Figure 8 The relations between residual phases on PS and the water levels. The horizontal axis indicates the data acquiring time. (a), (b) represents the residual phases of two typical PS on the top and bottom of the left part of the dam. The vertical axis indicates the residual phases, one radian represents 4.5mm deformation. The vertical axis in (c) indicates the water level differences between up- and downriver. The vertical axis in (d) indicates the upriver water levels. The three red dash lines indicate the time when water level difference reached peak values and divide the data acquisition time span into four parts indicated by the Roman numbers. The red triangle indicates the time when the cofferdam was dismounted.

4. AMPLITUDE ANALYSIS

According to Figure 4, the low coherence areas are mainly located in the middle and right parts of the dam and navigation establishments. Since the images were acquired during the construction of the dam, an amplitude matrix analysis is proposed to figure out the life spans of each target in different parts of the dam. Figure 9 shows the coherence matrices of four targets on the dam. Each pixel of a matrix identifies a pair of images. Blue indicates that the amplitude of the scatterer is similar in the two images, yellow and red mean that a change happened. Thus, from the amplitude matrix of the ship lift (Figure 9 (a)) it is possible to recognize the two states of the lift: up and down, that change the backscattered signal. The planthouses located on the right part of the dam were under construction during the data acquisition time, thus very few PS Candidate (PSC) can be detected. Nevertheless, the topography and deformation are still measured on the cofferdam. Moreover, some QPS are detected on the top of the spillway and navigation establishments. The results also prove the adaptability of the QPS technique in complicated situations.

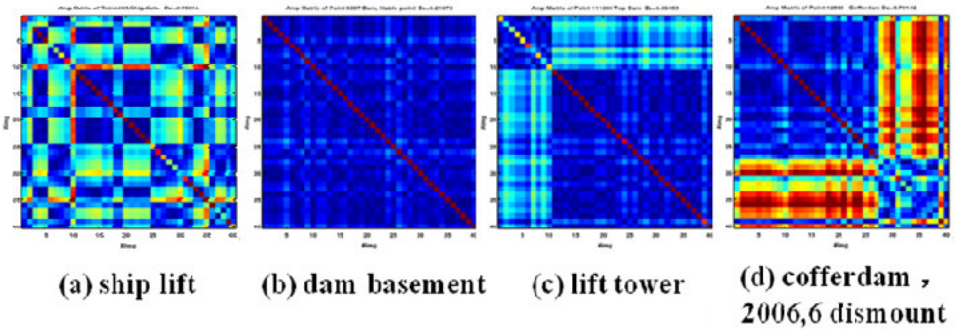

Figure 9 amplitude matrixes of four typical targets on the dam.

Many PSC are identified on the spillway, however, the estimated temporal coherence is very low. According to the amplitude analysis over the 40 SAR images, we found that there exist two states for the spillway, namely releasing and storing the water. When the sluice gates are open, the releasing water scatter the radar signal, very low amplitude can be observed in the corresponding SAR images and thus low temporal coherence can be obtained by QPS technique. The logarithm mean amplitude map with two different states are shown in Figure 10 (a) and (b). In Figure 10 (c) the difference between (a) and (b), focused on the spillway part, is shown. From Figure 10 (c), each sluice gate can be clearly observed due to their different reflective characteristics in the two different states. Till now, the number of images acquired when the gates are closed is not enough to carry out a reliable time series analysis and we could not obtain deformation estimates on the sluice gates. However, as soon as new data will be archived and high resolution SAR images will be available, the deformation measures on the right planthouses and on the spillway can also be expected from time series InSAR analysis.

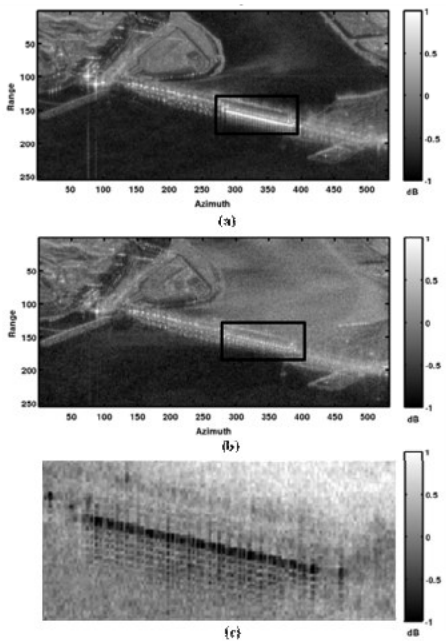

Figure 10 The logarithm mean amplitude map when the spillway was open or closed, and their difference. The spillway is indicated by the black rectangle. (a) the spill way is closed. (b) the spillway is open. (c) The enlarges vision of the differential image between (a) and (b).

5. CONCLUSIONS

Time series InSAR analysis allow us to extract terrain height and deformation trend with much higher coverage and density of measure points than conventional survey methods, as GPS or optical levelling. Thus time series InSAR analysis can be the best complement of conventional survey methods. The accuracy of time series InSAR techniques can be improved by control points provided by fieldwork,

and the density and coverage of monitoring points can be significantly improved by time series InSAR analysis. The combination of the two deformation estimates, namely, QPS and PS, allows us to monitor the stability at an acceptable cost and to identify risk areas. Recently, new generation satellites with higher resolution and shorter revisiting time have been launched allowing the estimate of more detailed and accurate information.

6. ACKNOWLEDGEMENTS

The authors would like to thank ESA for providing the SAR data through ESA-NRSCC Dragon II Cooperation Programme (id 5297) as well as Tele-Rilevamento Europa T.R.E. srl for focusing and registering the SAR data.

7. REFERENCES

[1] 申重阳, 孙少安, 刘少明, 项爱民, 李辉, and 刘光亮, "长江三峡库首区近期重力场动态变化," 大地测量与地球动力学, vol. 24, pp. 6-13, 2004.

[2] 李强, 赵旭, and 蔡晋安, "三峡水库坝址及邻区中上地壳P波速度结构," 中国科学D辑: 地球科学, vol. 39, pp. 427-436, 2009.

[3] 严建国, 李双平, "三峡大坝变形监测设计优化," 人民长江, vol. 33, pp. 36-38, 2002.

[4] A. Ferretti, C. Prati, and F. Rocca, "Permanent scatterers in SAR interferometry," Geoscience and Remote Sensing, IEEE Transactions on, vol. 39, pp. 8-20, 2001.

[5] C. Colesanti, A. Ferretti, F. Novali, C. Prati, and F. Rocca, "SAR monitoring of progressive and seasonal ground deformation using the permanent scatterers technique," Geoscience and Remote Sensing, IEEE Transactions on, vol. 41, pp. 1685-1701, 2003.

[6] A. Ferretti, G. Savio, R. Barzaghi, A. Borghi, S. Musazzi, F. Novali, C. Prati, and F. Rocca, "Submillimeter Accuracy of InSAR Time Series: Experimental Validation," Geoscience and Remote Sensing, IEEE Transactions on, vol. 45, pp. 1142-1153, 2007.

[7] D. Perissin, "Validation of the Sub-metric Accuracy of Vertical Positioning of PS's in C Band," Geoscience and Remote Sensing Letters, IEEE, vol. 5, pp. 502-506, 2008.

[8] D. Perissin, A. Ferretti, R. Piantanida, D. Piccagli, C. Prati, F. Rocca, F. de. Zan. and A. Rucci, "Repeat-pass SAR Interferometry with Partially Coherent Targets," in *Fringe07*, Frascati, Italy, 2007.

[9] 黄声享，尹晖，蒋征，变形监测数据处理 武汉大学出版社, 2004

[10] 戴会超，苏怀智， 三峡大坝深层抗滑稳定研究， 岩土力学，2006，vol. 27(4): pp. 643-647